

Anomalies in the transcriptional regulatory network of the yeast *Saccharomyces cerevisiae*

M. Tuğrul^{†*} and A. Kabakçioğlu[†]

[†] *Department of Physics, Koç University, Sarıyer 34450 Istanbul, Turkey*

^{*} *IFISC(CSIC-UIB) Institute for Cross-Disciplinary Physics and Complex Systems, Campus Universitat Illes Balears, E-07122 Palma de Mallorca, Spain*

Abstract

We investigate the structural and dynamical properties of the transcriptional regulatory network of the yeast *Saccharomyces cerevisiae* and compare it with two “unbiased” ensembles: one obtained by reshuffling the edges and the other generated by mimicking the transcriptional regulation mechanism within the cell. Both ensembles reproduce the degree distributions (the first -by construction- exactly and the second approximately), degree-degree correlations and the k -core structure observed in Yeast. An exceptionally large dynamically relevant core network found in Yeast in comparison with the second ensemble points to a strong bias towards a collective organization which is achieved by subtle modifications in the network’s degree distributions. We use a Boolean model of regulatory dynamics with various classes of update functions to represent in vivo regulatory interactions. We find that the Yeast’s core network has a qualitatively different behaviour, accommodating on average multiple attractors unlike typical members of both reference ensembles which converge to a single dominant attractor. Finally, we investigate the robustness of the networks and find that the stability depends strongly on the used function class. The robustness measure is squeezed into a narrower band around the order-chaos boundary when Boolean inputs are required to be nonredundant on each node. However, the difference between the reference models and the Yeast’s core is marginal, suggesting that the dynamically stable network elements are located mostly on the peripherals of the regulatory network. Consistently, the statistically significant three-node motifs in the dynamical core of Yeast turn out to be different from and less stable than those found in the full transcriptional regulatory network.

Key words: Boolean dynamics, attractor distribution, robustness, dynamical core network, canalizing functions
PACS: 89.75.-k, 64.60.Fr, 36.20.Ey

1. Introduction

Transcriptional regulatory network (TRN) describes the connective structure of the gene-gene interactions that regulate most physiochemical activities in a cell (Thomas, 1998; Albert & Barabási, 2002). This is particularly valid for *Saccharomyces cerevisiae* (from here on referred to as “Yeast”), an eukaryote which lacks miRNA and RNAi capability. Survival of the cell under changing external conditions requires both a responsive and a robust regulatory mechanism (Kauffman, 1993). The two key ingredients that contribute to the dynamics of regulatory activity are the network’s topology and the character of the regulatory interactions (Kauffman *et al.*, 2003). It is natural to attempt to identify the respective roles of these two components on the dynamical properties of the system. For this purpose, we consider here two neutral network ensembles and compare their representative members with the yeast’s transcriptional regulation network. The first ensemble (E1) is generated by reshuffling the edges on the Yeast’s TRN. This ensemble is suitable for identifying features that fall beyond those implied by the node connectivities. The second ensemble (E2) was developed in a recent study by Balcan *et al.* (2007) and was shown to mimic with high accuracy the global structural properties of the network of transcriptional regulatory interactions (Lee *et al.*, 2002; Teixeira *et al.*, 2006) found in Yeast. By comparing the characteristic features of the regulatory dynamics on Yeast’s TRN with those of the two ensembles, we discuss the relevance of in/out-degree statistics and the functional character of the interactions to the regulatory dynamics.

Below, we first focus on the structure of the TRN found in Yeast and those of the typical members of the two ensembles. Next, we investigate the differences between their dynamics in terms of their attractor statistics and robustness, both within the framework of a synchronous, Boolean time-evolution model.

2. Structure of Yeast’s TRN

A reasonably complete picture of the architecture of the TRN in Yeast is now available due to the collective effort of many experimental groups and

the recent development of high-throughput techniques (Spellman *et al.*, 1998; Lee *et al.*, 2002; Teixeira *et al.*, 2006). The structure is radically different from a random collection of 4252 nodes connected by 12541 edges, where the quoted numbers are those of the genes and known regulatory interactions in the YeastRACT database (Teixeira *et al.*, 2006) adopted by Balcan *et al.* (2007). In particular, the regulating nodes (transcription factors, or TFs) which constitute $\sim 3.5\%$ of all genes have a skewed out-degree distribution which has been suggested to follow a power-law (Guelzim *et al.*, 2002; Bergmann *et al.*, 2003; Maslov & Sneppen, 2005), and a roughly exponential in-degree distribution (Maslov & Sneppen, 2005), although the ranges of both distributions are somewhat narrow to make a strong case. Nevertheless, the deviation from a randomly wired network is strong and independent of the database used. A similar trend is observed in other structural aspects, such as degree-degree correlations and the k -core organization which appear to follow from the in- and out-degree distributions (Balcan *et al.*, 2007). Note that the numbers quoted above continue to increase as new experimental data pours in. However, for the sake of a fair comparison with the earlier study we stick to the same reference data and pay attention that our conclusions are based on observations (such as normalized distributions) that are likely to change little with further incoming data.

2.1. Reference ensembles

The ensemble E1 is an “unbiased” set of networks generated from Yeast’s TRN by shuffling the edges among the nodes while keeping the in- and out-degrees of each node unaltered. This is achieved simply by switching the end terminals of two randomly picked edges $(i \rightarrow j), (k \rightarrow l)$ to obtain two new edges $(i \rightarrow l), (k \rightarrow j)$, where we impose $i \neq j \neq k \neq l$ in order to keep the number of self-regulating genes fixed (see below). In spite of its frequent use in the literature, one should consider E1 a biologically inappropriate reference point. There is no good reason to assume that Nature selected Yeast’s TRN out of a pool of networks with identical degree distributions. Furthermore, such a reference simply ignores the question pertaining to the origin of the observed degree distribution for which several mechanisms have been proposed (Wagner, 1994; Van Noort *et al.*, 2004; Balcan *et al.*, 2007). Nevertheless, stastically significant deviations from E1 found in Yeast (features with a high z-score) allowed past studies to point out a high abundance of stability enhancing local motifs, such as feed-forward loops. On the other hand, the highest z-score 3-node motif thus found by Prill *et al.* (2005) can

be reproduced with the right frequency by means of a simple model which we also consider here to generate a second reference ensemble E2 as described below.

E2 is generated from a biologically motivated model introduced by Balcan *et al.* (2007). In this null model, two binary strings are associated with each yeast gene: first (S_1) representing the promoter site of the gene that regulates its transcription, second (S_2) representing the DNA sequence (motif) that the gene’s product binds. The lengths of the two sequences are chosen randomly from the associated length distributions determined from the available biological data provided by Harbison *et al.* (2004). A gene A is said to regulate gene B if $S_2^A \subset S_1^B$. No such B exists unless the product of A is a TF. For more details, we refer the reader to the original article.

Repeated generation of model networks with the same number of genes as in Yeast and different random number generator seeds forms the ensemble E2. Its typical members agree to very good accuracy with Yeast in terms of the in-, out-, and total-degree distributions, degree-degree correlation and the rich-club coefficient distributions. This ensemble further captures the hierarchical organization of Yeast’s TRN given by its k -core analysis, as well as the frequencies of most 3-node motifs observed in Yeast (see Section 4.3). Due to its success in simultaneously reproducing several distributional features of Yeast’s TRN from a single mechanism and *without any reference to the genetic sequence*, E2 appears a meaningful alternative to E1. It is a null-hypothesis constructed by a bottom-up approach, providing a microscopic explanation for a number of “anomalous” distributions observed in Yeast’s TRN and taken for granted in randomized ensembles such as E1. However, as shown below, even a quantitative agreement on those frequently quoted features may veil some significant differences between the actual Yeast and the two ensembles.

3. Dynamics

3.1. Boolean network model

Several methods can be employed for simulating the time evolution of gene expression within a cell (Norrell *et al.*, 2007). We here use a Boolean network model first proposed by Kauffman (1969), where the expression level $\sigma_i(t)$ of the i^{th} gene at time t is assumed 0 (silent) or 1 (expressed). The interaction between the regulatory genes and the regulated gene is deterministic and the

time evolution is synchronous, so that

$$\sigma_i(t+1) = F_i(\sigma_{j_1}(t), \sigma_{j_2}(t), \dots, \sigma_{j_{d_i}}(t)) ,$$

where d_i is the number of edges incoming to the node i (number of TFs regulating the i^{th} gene), $\{j_1, \dots, j_{d_i}\}$ are the nodes connected to i with incoming edges, and F_i is a Boolean function determining the state of gene i in presence of possibly multiple regulators.

Boolean dynamics of generic (such as, fixed in-degree (Kauffman, 1969), random (Aldana & Cluzel, 2003), power-law (Aldana, 2003)) networks have been of considerable interest for some time. Applications to biological systems include TRN models of *Arabidopsis thaliana* by Mendoza *et al.* (1999), *Drosophila melanogaster* by Albert & Othmer (2003), and the Yeast's cell-cycle network studied by Li *et al.* (2004). Unlike most past work which focused on part of the TRN associated with a particular function, we here focus on the *global* dynamical behavior of yeast and yeast-like regulatory networks. A recent work by (Lee & Rieger, 2007) in the same spirit compares Yeast and *E. coli* on a full-scale.

Determining the time evolution of the network starting from a given initial state is straightforward once the regulatory functions $\{F_i\}$ are fixed. However, the nature of these interactions in the actual organism are too complex and far from being well understood. Therefore, instead of attempting to identify the functions F_i that best describes the behavior of the yeast cell, we investigated the generic dynamical properties of the known architecture arising from a random choice of $\{F_i\}$ picked from a suitable collection.

It has been suggested that $\{F_i\}$ may be further restricted, based on the available experimental evidence, to certain subclasses of Boolean functions (Kauffman, 1993; Kauffman *et al.*, 2003; Nikolajewa *et al.*, 2007). These are

Simple Random Functions (RF): Each input is randomly assigned an output value of 1 with a probability p and 0 otherwise.

Canalizing Functions (CF): It has at least one canalizing input, say σ_{j_1} , such that $F_i(\sigma_{j_1} = \zeta, \dots) = s$. ζ and s are called the canalizing value and the canalized output, respectively (Kauffman, 1993). For consistency, we set $s = 1$ with probability p and let $F_i(\sigma_{j_1} = \bar{\zeta}, \dots)$ be a simple random function of the remaining variables.

Nested Canalizing Functions (NCF): Also called Hierarchical Canalizing Functions, they were proposed by Kauffman *et al.* (2003) based on an earlier

analysis due to Harris *et al.* (2002) and claimed to more closely mimic actual biological systems. All input variables of a NCF are canalizing and ordered in rank. The canalized output is determined by the highest ranking node at its canalizing value and is chosen to be 1 with probability p .

Special Nested Canalizing Functions (SNCF): Recently, gene regulation dynamics was observed to be consistent with a more restricted subclass of NCFs given by the Boolean expressions

$$\begin{aligned} & \tilde{\sigma}_{j_1} \wedge (\tilde{\sigma}_{j_2} \wedge (\dots \wedge (\tilde{\sigma}_{j_{d_i}-1} \wedge \tilde{\sigma}_{j_{d_i}})\dots)) \\ \text{and} \quad & \tilde{\sigma}_{j_1} \wedge (\tilde{\sigma}_{j_2} \wedge (\dots \wedge (\tilde{\sigma}_{j_{d_i}-1} \vee \tilde{\sigma}_{j_{d_i}})\dots)) \end{aligned} \quad (1)$$

where $\tilde{\sigma} \in \{\sigma, \bar{\sigma}\}$ and the probability of occurrence of the two functions were found to be 0.66 and 0.29, respectively (Nikolajewa *et al.*, 2007). The function classes above satisfy $\text{SNCF} \subset \text{NCF} \subset \text{CF} \subset \text{RF}$.

A constraint on these functions is that each input variable should be relevant, so that they have an experimentally detectable regulatory signature. Accordingly, for each input σ_{j_i} of a function F_i with d_i inputs, there exists at least one input set $\{\sigma_{j_1}, \dots, \sigma_{j_{d_i}}\}$, such that,

$$F_i(\sigma_{j_1}, \dots, \sigma_{j_i}, \dots, \sigma_{j_{d_i}}) \neq F_i(\sigma_{j_1}, \dots, \bar{\sigma}_{j_i}, \dots, \sigma_{j_{d_i}}) \quad (2)$$

with $\bar{\sigma} \equiv 1 - \sigma$. We ensure that the condition in Eq. (2) is satisfied in all cases.

Let π be the fraction of inputs to F_i that satisfy Eq. (2) for which the output equals 1 calculated over all genes:

$$\pi = (1/N) \sum_i \delta_{F_i(\sigma_{i_1}, \dots, \sigma_{i_{d_i}}, 1)/2^{d_i}} \quad (3)$$

with $N =$ total number of genes and $\delta_{i,j}$ is the Kronecker delta function. For the SNCF class, π is not a free parameter but determined by the in-degree distribution of the network. For the rest of the function types we have $\pi \neq p$ in general, because Eq. (2) filters out some function assignments. In fact, the fraction ϕ_n of the Boolean functions satisfying Eq. (2) with n inputs is well-known (Harrison, 1965):

$$\begin{aligned} \phi_1 &= 2/4 \\ \phi_2 &= 10/16 \\ \phi_3 &= 218/256 \\ \phi_4 &= 64594/65536 \end{aligned} \quad (4)$$

where the denominators are 2^{2^n} : number of Boolean functions with n inputs. For a fair comparison (except in the discussion on robustness), we adjusted the parameter p for RF, CF, and NCF, so that $\pi \simeq 0.29$, the value one obtains both for Yeast and the two ensembles with a SNCF assigned to each gene.

We will compare the impact of each function class on the system’s dynamics when implemented on the dynamically relevant core network of the TRN described in the next section.

3.2. Dynamically Relevant Core

The number of the dynamical attractors in a Boolean network is determined by a *dynamically relevant core* network (DRC) involving TFs only. DRC in Yeast is much smaller than the full transcriptional regulatory network and allows one to perform time-efficient simulations of the regulatory dynamics.

[Figure 1 about here.]

We define a global DRC for Yeast by recursively pruning all the nodes with zero in-degree or zero out-degree (see Fig. 1). Most of the genes in the transcriptional regulatory network of Yeast are “slave” genes that do not take part in the regulation process or do so merely in a downstream fashion. Their presence may effect the transient behavior or the size of the dynamical cycles the network eventually falls into, however they do not change the number of distinct steady-states (or attractors, see below) and their probabilities of occurrence under different function assignments. These genes can be pruned by recursively eliminating nodes with zero out-degree.

In a similar fashion there exist a set of genes with zero in-degree, whose expression levels remain unchanged throughout the dynamics. Some of these are ‘housekeeping’ genes that are always expressed to perform routine functions (such as RNA production) while others are fixed by the environmental conditions. We will consider the regulatory dynamics when the states of these genes are fixed and prune them as well, assuming that the averaging over different state assignments to such genes is properly accounted for by different function assignments on the remaining network. See the recent work by Lee & Rieger (2007) for an earlier implementation of this procedure on Yeast, while for a different reductionist approach see Paul *et al.* (2006).

[Figure 2 about here.]

The end product (shown in Fig. 2 for Yeast) is a subnetwork where each node is a TF regulated by other genes in the DRC and/or by itself. Given that only 3.5% of all the genes in *Saccharomyces cerevisiae* are TFs, described pruning process brings a sizeable reduction in the computation time. We found that Yeast’s dynamically relevant subnetwork contains 82 TF genes and 254 interactions between them.

Comparison of DRC sizes in Yeast vs reference ensembles

[Figure 3 about here.]

We also obtained the DRC for 1000 networks chosen from each ensemble. In the case of E2, ensuring that the samples before pruning have, on average, the same number of nodes and edges as Yeast’s TRN . The comparison of the three cases is shown in Fig. 3. The outcome is instructive: The distribution of the DRC size on E2 shows a big contrast with Yeast while the agreement with the edge-reshuffled ensemble E1 (with *exactly* the same in- and out-degrees at each node) is perfect when self-regulating genes are included and still better than E2 otherwise. (See next section for a discussion on self-regulating genes.) A similar situation is observed also for the number of interactions in the DRC. In view of the quantitative agreement of in- and out- degree-distributions between Yeast and E2 (Balcan *et al.*, 2007), this result points to a subtle difference between the two ensembles that translates into a three-fold size difference in the respective DRCs.

There is no doubt that, a complete model of the regulatory dynamics should include the environmental inputs carried by the signaling pathways and the post-transcriptional regulatory interactions (Thomas, 1998; Samal & Jain, 2008). Accordingly, a complete DRC should include of both TFs and non-TF proteins (see, e.g. Li *et al.* (2004)). Nevertheless, the “transcriptional regulatory” DRC defined as above remains an intrinsic property of the organism, which in the case of Yeast appears to be significantly out of proportion.

3.3. Number of Attractors

The dynamical characterization of a TRN is complete once all the interactions (the network’s architecture) and the update functions $\{F_i\}$ of all genes are specified. The network state $S(t) \equiv \{\sigma_1(t), \sigma_2(t), \dots, \sigma_N(t)\}$ at the discretized time $t = n\Delta t$ after n update cycles can be expressed symbolically

as

$$S(t) = F^n(S(0)) . \quad (5)$$

The time unit Δt is assumed to be large enough to encompass all protein production related processes. Since the time evolution is deterministic, the number of possible dynamical trajectories is 2^N , i.e., the number of distinct initial conditions. 2^N is also the size of the state space, therefore each initial condition eventually ends up in a cycle which is called the *attractor* for that initial state. A state S_k is a member of the attractor if and only if $S(t + n\Delta t) = S(t) = S_k$ for some integer $n > 0$. Minimal such n is called the *length* of the attractor cycle. The attractor is a *fixed point* if $n = 1$ and a *limit-cycle* otherwise. Note that the attractor lengths (except those of the fixed points) are modified after the pruning process describe above, but the number of attractors is not. Therefore we focus on the statistics of their number below.

We note in passing that, the attractors of a transcriptional regulation network may be associated with the observable features of the organism. For example, the expression pattern of the segment polarity genes in *Drosophila melanogaster* can be mapped to the fixed point of the relevant regulatory subnetwork (Albert & Othmer, 2003). In *Arabidopsis thaliana*, the attractors of the regulatory subnetwork responsible from cell differentiation have been shown to correspond to different phenotypes (Mendoza *et al.*, 1999).

The number of attractors, N_{att} , remains invariant as we switch from the full-size network to the DRC, but estimating its exact value is difficult due to the vast number of initial conditions that should be checked. However, by randomly sampling a small number of initial conditions, another - and possibly more relevant - measure of the number of attractors, \tilde{N}_{att} , can be easily calculated. \tilde{N}_{att} is obtained by properly weighting the i^{th} attractor by its *basin of attraction* ω_i , the number of initial conditions that end up in i . This procedure allows one to distinguish between, e.g. two network realizations (network + function assignments) with two attractors each, whose relative basin sizes are (0.99, 0.01) in the first case and (0.5, 0.5) in the second. It is fair to say that the first network realization has a single dominant attractor, while the second one has two. The generalization of this argument gives $\tilde{N}_{att} = 2^S$, where S is the standard dynamical entropy of the network (see, e.g., Krawitz & Shmulevich (2007)):

$$S = - \sum_i p_i \log_2 p_i \quad (6)$$

where $p_i = \omega_i/2^N$ is the probability that a uniformly selected initial condition is in the basin of attraction of the i^{th} attractor. Note that $\tilde{N}_{att} \leq N_{att}$. The difference between the two attractor counts is demonstrated in Fig. 4 over the E2 ensemble.

[Figure 4 about here.]

We estimated the average number of attractors for Yeast’s DRC and the model DRCs. Since an exact enumeration is out of question with 2^{82} possible initial states (and unnecessary for estimating \tilde{N}_{att}), we randomly sampled 1000 initial conditions and followed their trajectories in time until an attractor was reached. The attractor was then characterized by the sequence of states in the cycle (or by the state id for fixed points) and the number of initial conditions that end up in each state were counted.

\tilde{N}_{att} thus found for the networks were further averaged over 1000 different structures, with each structure analyzed using 10 independent Boolean function assignments chosen from each of the classes above. Mean attractor numbers thus found for the E2 ensemble are 2.3, 2.2, 2.3 and 1.9 when the update functions were chosen from the classes RF, CF, NCF and SNCF, respectively. We deliberately omitted the error bars in the values reported above, because the distribution of the attractor number is highly skewed and has a fat tail, as shown in Fig. 4. A fair comparison with Yeast and E1 requires some more work and is presented below. However, except for a somewhat smaller average attractor count observed for SNCFs, neither on Yeast nor on the reference ensembles did we find a significant difference among the attractor statistics of different function classes.

3.4. *Robustness of the dynamics*

The survival of a cell relies on the continuously and reliable production of a vast amount of proteins in proper quantities. Therefore, the “equilibrium” gene expression profile (encoded here by an attractor) is expected to possess a certain level of stability, i.e., robustness to perturbations such as random fluctuations in expression levels or temporary malfunction of a gene. On the other hand, a certain level of responsiveness is also necessary in order to be able to cope with the environmental changes in longer time scales. This trade-off suggests that living organisms function in the vicinity of the order-chaos boundary, a hypothesis originally formulated by Kauffman (1993).

A dynamical system is said to be chaotic if a small perturbation introduced into one of its two, otherwise identical, copies drives them away from

each other exponentially fast. Adopted to TRN dynamics, this amounts to monitoring in time the normalized “Hamming distance”

$$h(S, S') = (1/N) \sum_i^N [\sigma_i - \sigma'_i]$$

between the two copies S and S' . The network’s robustness is then determined by

$$r = \lim_{h \rightarrow 0^+, t \rightarrow \infty} \langle dh(t + \Delta t) / dh(t) \rangle, \quad (7)$$

where the first limit ensures that the measured quantity is a steady-state property (a function of the attractors only), the second reflects that r is a linear response function. Δt is chosen to be a small time interval (one time step in our case) and the averaging is over possible perturbations (Aldana, 2003). The network is said to be chaotic if $r > 1$ and ordered if $r < 1$ (both in an average sense, for there may be particular perturbations in each case that result in the opposite behavior.) We will show below that, RF, CF, NCF and SNCF display significant variability in robustness on the Yeast and the model networks.

4. Yeast *vs* model networks

4.1. Attractor statistics

Performing the same analysis on Yeast’s TRN and E1, one finds that the average number of attractors is orders of magnitude larger for RF type functions. In fact, most of the initial conditions end up in different attractors, so that \tilde{N}_{att} is capped by the number of initial conditions used for averaging. Such disagreement is too large to be explained by the mismatch in DRC sizes shown in Fig. 3. For an estimate of the network-size dependence of N_{att} see, e.g., Drossel (2005) and Balcan & Erzan (2006).

Upon closer inspection, the excessive attractor number turns out to be due to another structural anomaly in Yeast: the presence of a large number of self-regulating genes. 16% of all genes in the DRC (13 out of 82) are self-regulating (Teixeira *et al.*, 2006) as opposed to 5% (less than 2 out of an average of 35.6 - see Fig. 3) in E2 model. Note that a self-regulating gene is by definition a member of the DRC and is preserved under the edge shuffling process used for generating E1 networks. Each such node under synchronous Boolean dynamics potentially doubles the attractor count due

to a parity effect. The excess of such nodes in Yeast’s TRN is well known (see, e.g., (Lee & Rieger, 2007)), although it can easily be missed in a structural comparison as in Balcan *et al.* (2007) unless specifically looked for. Its dynamical signature, however, is difficult to overlook. This example serves as a demonstration for how a comparative study of the dynamics may lead to the discovery of structural features specific to Yeast.

We next eliminate the self-loops from Yeast and both model networks, and reconstruct the DRCs. By doing so, we temporarily depart from a faithful representation of Yeast. On the other hand, we ensure that further discrepancies we may encounter originate from structural differences other than the high frequency of self-regulating genes in Yeast. The self-interactions will be restored in the next section.

[Table 1 about here.]

Interestingly, the histograms $p(\tilde{N}_{att})$ obtained from Yeast now differ significantly from those of both reference ensembles. Fig. 5 displays the contrast for RF type functions, while qualitatively the same picture is obtained also for other function classes. Majority of E1 and E2 model networks are dominated by a single attractor, while Yeast’s DRC typically has multiple attractors and a nonmonotonous $p(\tilde{N}_{att})$. The contrast between the average attractor numbers is shown in Table 1. The tail of the attractor number distribution obtained from Yeast is also markedly different, as shown in the inset of Fig. 5.

[Figure 5 about here.]

It is not possible to understand this dynamical anomaly of Yeast in terms of the difference in the DRC sizes shown in Fig. 3. Because, first, the mismatch in \tilde{N}_{att} persists between E1 and Yeast which have identical DRC sizes. Second, although a smaller “random” network is expected to have a smaller number of attractors on average (Drossel, 2005; Balcan & Erzan, 2006), we observed above that E1 and E2 networks (without self-regulating nodes) which have approximately a factor of two size difference come with almost the same number of attractors. We further confirmed this second observation by repeating our analysis on a filtered subset of E2 networks (again, without self-loops) whose number of TFs and the number of interactions in the DRC are within 5% of Yeast’s. \tilde{N}_{att} is essentially the same as before (also shown in Fig. 5). Therefore, we conclude that

1. Synchronous Boolean dynamics on DRC-type networks has an attractor

statistics with a much weaker size dependence than random networks,
 2. Yeast’s TRN has certain structural elements that amount to a significant modification of its attractor statistics and are not captured by either of the two model ensembles E1 & E2.

4.2. Robustness

We performed the analysis outlined above on Yeast and also on E1 and E2 networks with similar DRC sizes (and with self-interactions untouched) as described earlier. We found that, the robustness depends significantly on the type of the update function: the more restrictive the function set, the more robust is the dynamics (see Fig. 6). Maybe more relevant is the fact that, under fully random functions (RF) Yeast’s regulatory dynamics is chaotic for a wide range of p values. In contrast, the nested canalizing functions ensure that the dynamics is stable, although it may be functioning close to the order-chaos boundary if one effectively has $p \simeq 1/2$.

[Figure 6 about here.]

It is worthwhile pointing out that, results in Fig. 6 differ from the approximate analytical form formulated by Aldana (2003) and Derrida & Pomeau (1986):

$$r = 2\langle k \rangle p(1 - p) , \tag{8}$$

where $\langle k \rangle$ is the average in-degree of the network. The disagreement is due to the condition given in Eq. (2). This experimentally imposed constraint renders the system relatively less robust with respect to an unbiased choice of the update functions, because functions filtered by Eq. (2) are insensitive to at least one of the input variables. As a result, the range of the robustness measure r is squeezed into a narrower interval around the order-chaos boundary $r = 1$, conforming to the edge-of-chaos hypothesis of Kauffman (1993). Furthermore, as seen in Eq. (4), the constraint in Eq. (2) is not equally restrictive on all nodes. For example, a node with $k = 1$ has $\pi_1 = 1/2$ independent of input value p , whereas for $k \gtrsim 5$ we have $\pi_k \simeq p$. Generalizing Eq. (8) accordingly, we obtain

$$r(p) = \sum_k 2k n(k) \pi_k(p) [1 - \pi_k(p)] , \tag{9}$$

where $n(k)$ is the fraction of nodes with in-degree k . $\pi_k(p)$ on the RF class is shown in Fig. 7. The CF and NCF classes give qualitatively similar behavior.

The prediction of Eq. (9) on model networks with the RF-type functions is also plotted in Fig. 6 for comparison.

[Figure 7 about here.]

Finally, lifting the constraint of Eq. (2) recovers the expected trend in Eq. (8) for Yeast with RF assignments (Tuğrul & Kabakçioğlu, 2009), while the relative order of robustness among different function types is preserved (not shown).

4.3. Motifs

Regulatory networks are known to exhibit an abundance of certain subgraphs (Milo *et al.*, 2002). Prill *et al.* (2005) list the high frequency subgraphs for several organisms by comparing the TRN with an ensemble obtained by reshuffling the edges while keeping the *total degree* of each node fixed. They establish a connection between the network structure and its dynamics through the stability properties of each motif. In particular, the motifs (b),(f) and (g) in Table 2 were found relatively abundant (with a high z-score) in Yeast.

A similar investigation comparing Yeast’s (unpruned) TRN with the two reference ensembles E1 & E2 was reported earlier in Supplement 1 of (Balcan *et al.*, 2007) and is worth re-examining here. Interestingly, the relatively high content of the motif (b) in Table 2 reported by (Prill *et al.*, 2005) is found to be reproduced not only by E1 but also by the E2 ensemble (the relative frequency of the motif’s occurrence is 96.4% in the *unpruned* Yeast and E1 networks and 97.0% in E2). Therefore, this feature should be associated with the basic matching mechanism of the transcriptional regulation process exploited in E2, and its high occurrence rate in Yeast is guaranteed by the in- and out-degree statistics (hence the agreement with E1) that is encoded into the transcription factor binding sequence statistics.

On the other hand, cascaded regulation motif (a) and the feed-forward loop motif (f) of Table 2 appear respectively $\sim 50\%$ and $\sim 80\%$ more frequently in the unpruned Yeast network relative to E2. The excess of these two motifs in Yeast therefore require a different explanation, such as the stability considerations given by (Prill *et al.*, 2005).

[Table 2 about here.]

The discrepancy in the attractor statistics (or the lack of it in respective robustnesses) observed between Yeast and the reference model DRCs are likely to be related to their motif statistics. On the other hand, there is no a priori reason that the motif frequencies on the unpruned network quoted above should also apply to the DRC. Therefore we performed a similar analysis on the core networks of Yeast, E1 and E2 using *Mfinder*, the free motif-finder software from Alon Lab (Kashtan *et al.*, 2004). The results are shown in Table 2.

Interestingly, the strong bias towards an excess of dynamically stable motifs such as (b) and (f) in Yeast does not persist in the DRC. At the same time, (d) and (e) in Table 2 involving mutually regulating TF pairs are 60-350% more frequent in Yeast in comparison to reference DRCs. These two motifs were labelled as partially stable by (Prill *et al.*, 2005). Our results on network robustness shown in Fig. 6, where no significant difference can be seen between Yeast and the reference models under Boolean dynamics, are consistent with such motif statistics.

5. SUMMARY and DISCUSSION

We have investigated the dynamical properties of Yeast’s transcriptional regulatory network by means of Boolean functions with parallel (synchronous) update rules and compared them with two null-models that capture many of the global structural features found in Yeast. We found that, the core of the Yeast network (DRC) that determines the steady-state features of the dynamics is much larger than the unbiased model (E2) whose sole premise is that the regulation mechanism is based on sequence-specific binding of transcription factors.

Comparison of the average number of attractors (properly weighted by the basin size) reveals not only the well-known abundance of many self-regulating genes, but also further differences between the Yeast and model networks. In particular, we find that the architecture of the Yeast DRC typically permits several attractors, whereas the model networks -even after the differences in the number of self-regulating TFs and the core network sizes are eliminated- come typically with a single attractor. The tail of the attractor number distribution in Yeast is also noticeably different. An important question is whether these features survive under a more realistic asynchronous time-evolution model, although our observations relating to the network structure remain valid independent of this choice.

A comparison of the network stability under minor perturbations reveals that the Yeast’s dynamical core is *not* more robust than either of the two reference models, in (apparent) contrast with earlier results. This observation is also supported by the presence of a different set of 3-node motifs that are found in relatively high proportions in Yeast when the DRC (rather than the whole regulatory network) is taken into account. The significantly frequent motifs in the DRC are dynamically less stable than those found in abundance in the full TRN of Yeast.

Upon visual inspection, it is not all too unexpected that the stable motifs (a-c)&(f) are found mostly on the “peripherals” of the network eliminated by the pruning process. However, it is interesting to observe how topology itself supports the robustness-responsiveness dichotomy in transcriptional regulation process. Robustness is associated with the peripheral components that carry the environmental signals downstream, i.e., small variations are filtered out before they reach the DRC. On the other hand, DRC itself is relatively more responsive than the embedding network to changes in the expression levels of its constituent genes. Favorably so, since such changes are likely to reflect shifts in operational conditions that are persistent enough to survive the downstream filtering.

Acknowledgements

We would like to thank A. Erzan, M. Mungan and D. Balcan for valuable discussions that led to the present work and a critical reading of the manuscript. We appreciate the help of D. Balcan for providing the model networks at an initial stage. This project was supported by TUBITAK through the grant TBAG-106T553.

References

- ALBERT, R. & BARABÁSI, A. L. (2002). Statistical mechanics of complex networks. *Rev. Mod. Phys.* **74**(1), 47–97.
- ALBERT, R. & OTHMER, H. G. (2003). The topology of the regulatory interactions predicts the expressions pattern of the segment polarity genes in drosophila melanogaster. *Journal of Theoretical Biology* **223**, 1–18.
- ALDANA, M. (2003). Boolean dynamics of networks with scale-free topology. *Physica D* **185**, 45–66.

- ALDANA, M. & CLUZEL, P. (2003). A natural class of robust networks. *PNAS* **100**(15), 8710–8714.
- BALCAN, D. & ERZAN, A. (2006). Dynamics of content based networks. In: *ICCS 2006, Part III, LNCS 3993* (ET AL., V. N. A., ed.), Springer-Verlag. Berlin.
- BALCAN, D., KABAKÇIOĞLU, A., MUNGAN, M. & ERZAN, A. (2007). The information coded in the yeast response elements accounts for most of the topological properties of its transcriptional regulation network. *PLoS ONE* **2**(6), e501.
- BERGMANN, S., IHMELS, J. & BARKAI, N. (2003). Similarities and differences in genome-wide expression data of six organisms. *PLOS Biology* **2**(1), 1–9. [Www.plosone.org](http://www.plosone.org).
- DERRIDA, B. & POMEAU, Y. (1986). Random networks of automata: A simple annealed approximation. *Europhysics Letters* **1**(2), 45–49.
- DROSSEL, B. (2005). Number of attractors in random boolean networks. *Phys. Rev E* **72**, 016110.
- GUELZIM, N., BOTTANI, S., BOURGINE, P. & KEPES, F. (2002). Topological and causal structure of the yeast transcriptional regulatory network. *Nature Genetics* **31**, 60–63.
- HARBISON, C., GORDON, D., LEE, T., RINALDI, N., MACISAAC, K. & ET. AL. (2004). Transcriptional regulatory code of a eukaryotic genome. *Nature* **431**, 99–104.
- HARRIS, S. E., SAWHILL, B. K., WUENSCH, A. & KAUFFMAN, S. (2002). A model of transcriptional regulatory networks based on biases in the observed regulation rules. *Complexity* **7**(4), 23–40.
- HARRISON, M. A. (1965). *Introduction to Switching and Automata Theory*. McGraw Hill, NY.
- KASHTAN, N., ITZKOVITZ, S., MILO, R. & ALON, U. (2004). Efficient sampling algorithm for estimating subgraph concentrations and detecting network motifs. *Bioinformatics* **20**(11), 1746–1758.

- KAUFFMAN, S. A. (1969). Metabolic stability and epigenesis in randomly connected nets. *Journal Of Theoretical Biology* **22**, 437.
- KAUFFMAN, S. A. (1993). *The Origins of Order*. Oxford University Press, 1 ed.
- KAUFFMAN, S. A., PETERSON, C., SAMUELSSON, B. & TROEIN, C. (2003). Random boolean network models and the yeast transcriptional network. *PNAS* **100**(25), 14796–14799.
- KRAWITZ, P. & SHMULEVICH, I. (2007). Basin entropy in boolean network ensembles. *Physical Review Letters* **98**(15), 158701.
- LEE, D. & RIEGER, H. (2007). Comparative study of the transcriptional regulatory networks of *E. coli* and yeast: Structural characteristics leading to marginal dynamic stability. *Journal of Theoretical Biology* **248**(4), 618–626.
- LEE, T. I., RINALDI, N. J., ROBERT, F., ODOM, D. T., BAR-JOSEPH, Z., GERBER, G. K., HANNETT, N. M., HARBISON, C. T., THOMPSON, C. M., SIMON, I., ZEITLINGER, J., JENNINGS, E. G., MURRAY, H. L., GORDON, D. B., REN, B., WYRICK, J. J., TAGNE, J. B., VOLKERT, T. L., FRAENKEL, E., GIFFORD, D. K. & YOUNG, R. A. (2002). Transcriptional regulatory networks in *saccharomyces cerevisiae*. *Science* **298**(5594), 799–805.
- LI, F., LONG, T., LU, Y., OUYANG, Q. & TANG, C. (2004). The yeast cell-cycle network is robustly designed. *PNAS* **101**(14), 4781–4786.
- MASLOV, S. & SNEPPEN, K. (2005). Computational architecture of the yeast regulatory network. *Phys. Biol.* **2**(4), S94–S100.
- MENDOZA, L., THIEFFRY, D. & ALVAREZ-BUYULA, E. (1999). genetic control of flower morphogenesis in *arabidopsis thaliana*: a logical analysis. *Bioinformatics* **15**(7/8), 593–606.
- MILO, R., SHEN-ORR, S., ITZKOVITZ, S., KASHTAN, N., CHKLOVSKII, D. & ALON, U. (2002). Network motifs: simple building blocks of complex networks. *Science* **298**(5594), 824–827.

- NIKOLAJEWA, S., FRIEDEL, M. & WILHELM, T. (2007). Boolean networks with biologically relevant rules show ordered behavior. *BioSystems* **90**(1), 40–47.
- NORRELL, J., SAMUELSSON, B. & SOCOLAR, J. E. S. (2007). Attractors in continuous and Boolean networks. *Phys. Rev. E* **76**(4), 046122.
- PAUL, U., KAUFMAN, V. & DROSSEL, B. (2006). Properties of attractors of canalizing random boolean networks. *Phys. Rev. E* **73**, 026118.
- PRILL, R. J., IGLESIAS, P. A. & LEVCHENKO, A. (2005). Dynamic properties of network motifs contribute to biological network organization. *PLOS Biology* **3**(11), 1881–1892.
- SAMAL, A. & JAIN, S. (2008). The regulatory network of e. coli metabolism as a boolean dynamical system exhibits both homeostasis and flexibility of response. *BMC Systems Biology* **2**(21), 1–18.
- SPELLMAN, P. T., SHERLOCK, G., ZHANG, M. Q., VISHWANATH, R., ANDERS, K., EISEN, M. B., BROWN, P. O., FUTCHER, B. & FINK, G. R. (1998). Comprehensive identification of cell cycle-regulated genes of the yeast *saccharomyces cerevisiae* by microarray hybridization. *Molecular Biology of the Cell* **12**, 3273–3297.
- TEIXEIRA, M. C., MONTEIRO, P., JAIN, P., TENREIRO, S., FERNANDES, A. R., MIRA, N. P., ALLENQUER, M., FREITAS, A. T., OLIVEIRA, A. L. & CORREIA, I. S. (2006). The yeasttract database: a tool for the analysis of transcription regulatory associations in *saccharomyces cerevisiae*. *Nucl. Acids Res.* **34**, D446–D451.
- THOMAS, R. (1998). Laws for the dynamics of regulatory networks. *Int. J. Dev. Biol.* **42**, 479–485.
- TUĞRUL, M. & KABAKÇIOĞLU, A. (2009). Robustness of transcriptional regulation in yeast-like model boolean networks. *International Journal of Bifurcation and Chaos* Accepted.
- VAN NOORT, V., SNEL, B. & HUYNEN, M. (2004). The yeast coexpression network has a small-world, scale-free architecture and can be explained by a simple model. *EMBO reports* **5**(3), 280.

WAGNER, A. (1994). Evolution of gene networks by gene duplications: a mathematical model and its implications on genome organization. *Proceedings of the National Academy of Sciences* **91**(10), 4387–4391.

CAPTIONS

Figure 1: **Extraction of DRC.** A depiction of the pruning procedure used for extracting the dynamically relevant core of Yeast. Numbers refer to the stage of the recursive process at which the nodes/edges are removed. The red edges are the interactions left in the DRC.

Figure 2: **DRC of Yeast.** The dynamically relevant subnetwork of the Yeast’s TRN obtained by the pruning procedure described above.

Figure 3: **DRC sizes: models vs. Yeast.** The probability distribution function of the number of genes in the DRC with (red and blue) and without (green and black) self-regulating genes.

Figure 4: **Bare vs. weighted attractor count.** The difference between the probability distribution functions for N_{att} (full) obtained by plain counting and \tilde{N}_{att} (empty) defined in the text reflects the network’s preference towards an uneven basin-size distribution. (By Eq. (6), $\tilde{N}_{att} = N_{att}$ if attractors have equal basin sizes.) Presented data is obtained from the E2 ensemble only for reasons discussed in the text.

Figure 5: **Number of attractors: models vs. Yeast.** Probability distribution functions for the number of attractors in Yeast (\circ) vs. model ensembles with update rules of type RF after the self-loops are removed. Data obtained from E1 (\square) and E2 (\diamond) ensembles are shown together with those over a subset of the E2 networks whose DRC sizes are in the same ballpark as that of Yeast’s (\triangle). Inset shows the tails of the distributions on a log-log scale. Unit size bins were used for the histograms.

Figure 6: **Robustness of Yeast and model networks.** Robustness of Yeast vs. model networks with equal DRCs. Horizontal axis spans $0 \leq p \leq 0.5$, since $r(p)$ in Eq. (7) is symmetric with respect to $p = 0.5$. Shaded regions indicate the range within one standard deviation of E1 (red) and E2 (blue) reference results. Solid curves represent Yeast. Horizontal dashed line is the border between ordered and chaotic behavior. Dotted curve corresponds to the theoretical prediction for the RF case obtained from Eq. (9).

Figure 7: **Impact of the “relevance” condition.** The unconditional probability $\pi_k(p)$ for a node with in-degree k to be 1 obtained when the Random Boolean functions (RF) with bias p are subjected to the constraint in Eq. (2). These functions are fed into Eq. (9) in order to obtain an analytical estimate for the network robustness. The larger the deviation from the diagonal the stronger is the impact of the constraint.

Table 1: **Average attractor number.** Average attractor number obtained for each function class on the DRC of the Yeast and the two reference ensembles. E2* refers to the E2 ensemble networks which have the same DRC size as Yeast.

Table 2: **3-node Motif statistics.** Top 3-node motifs ordered according to their frequency of appearance in Yeast DRC. Lower percentages are those obtained from model networks with the same DRC size as Yeast’s.

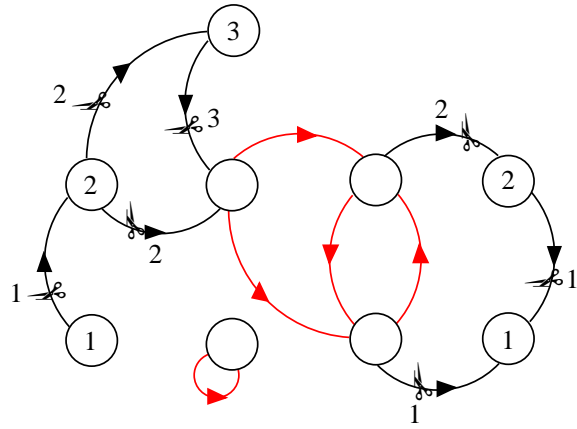


Figure 1:

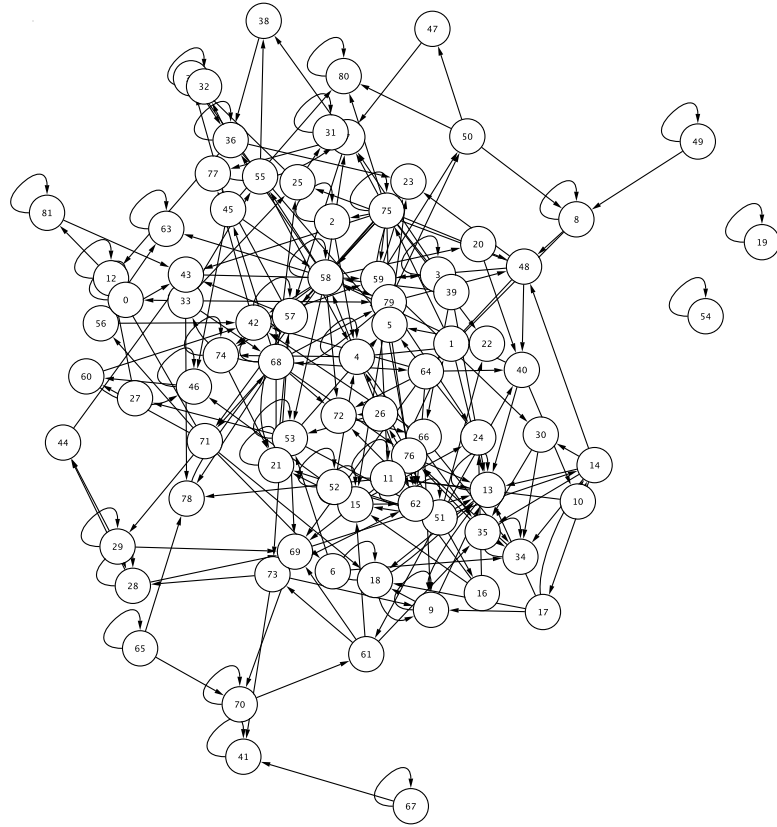


Figure 2:

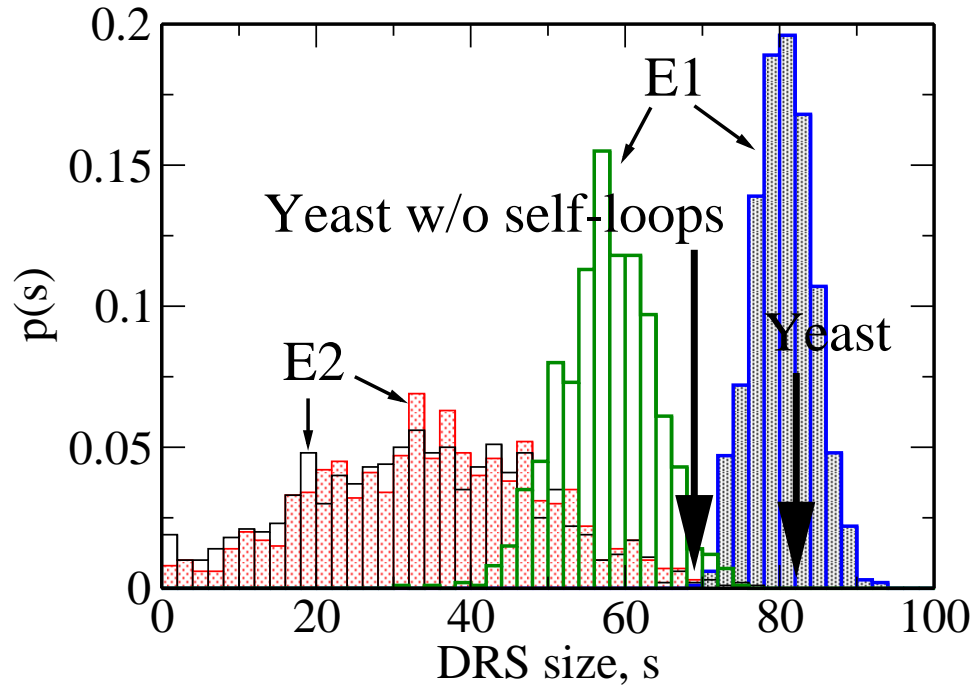


Figure 3:

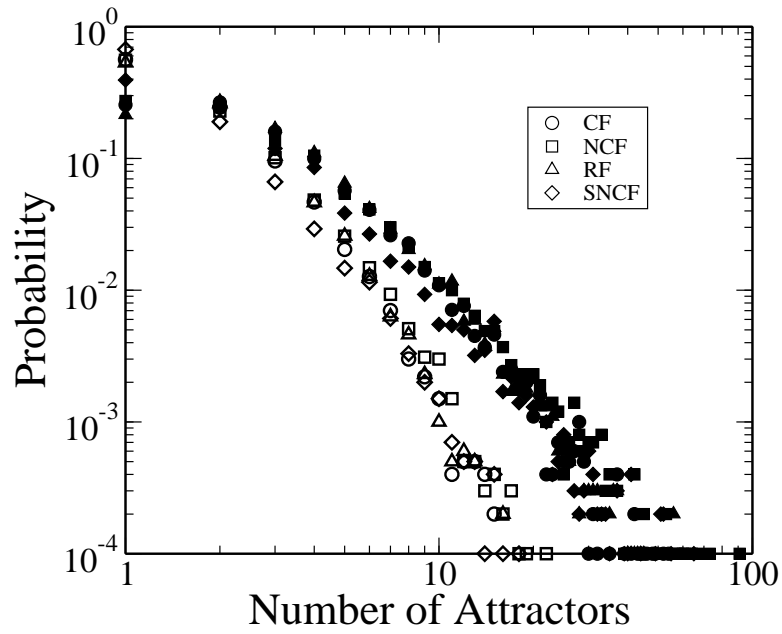


Figure 4:

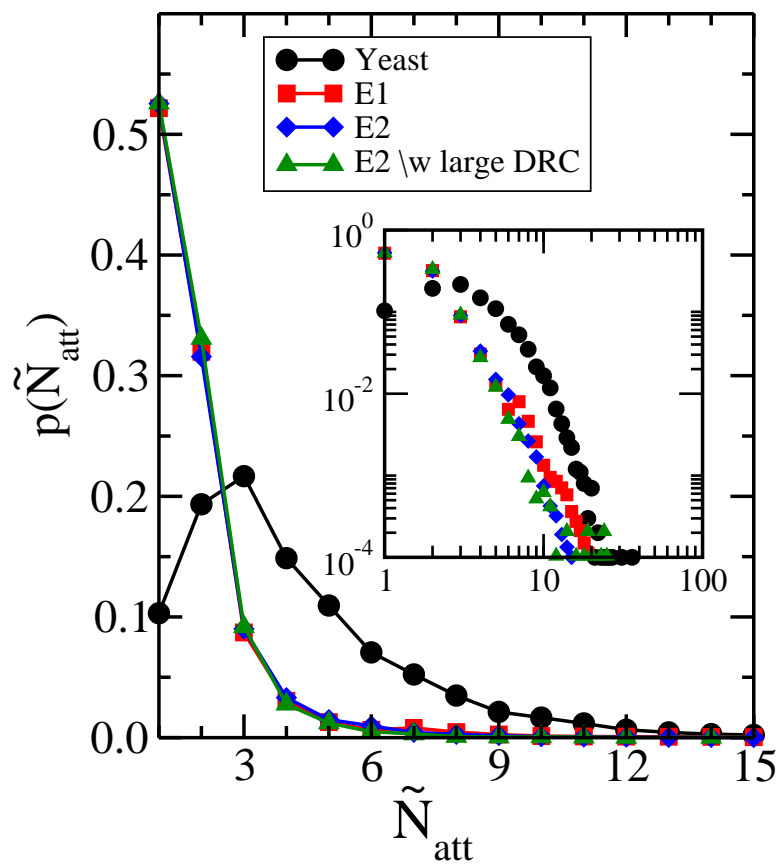


Figure 5:

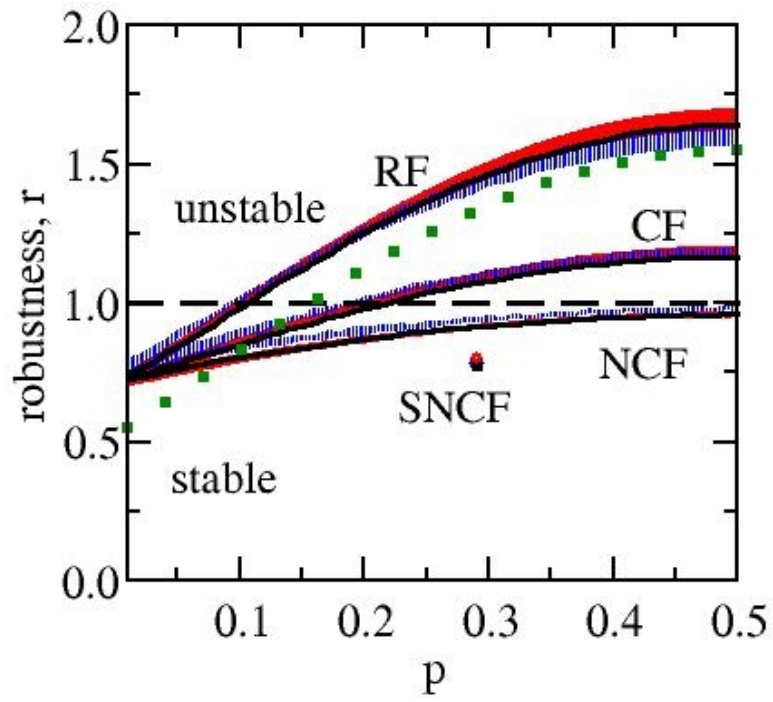


Figure 6:

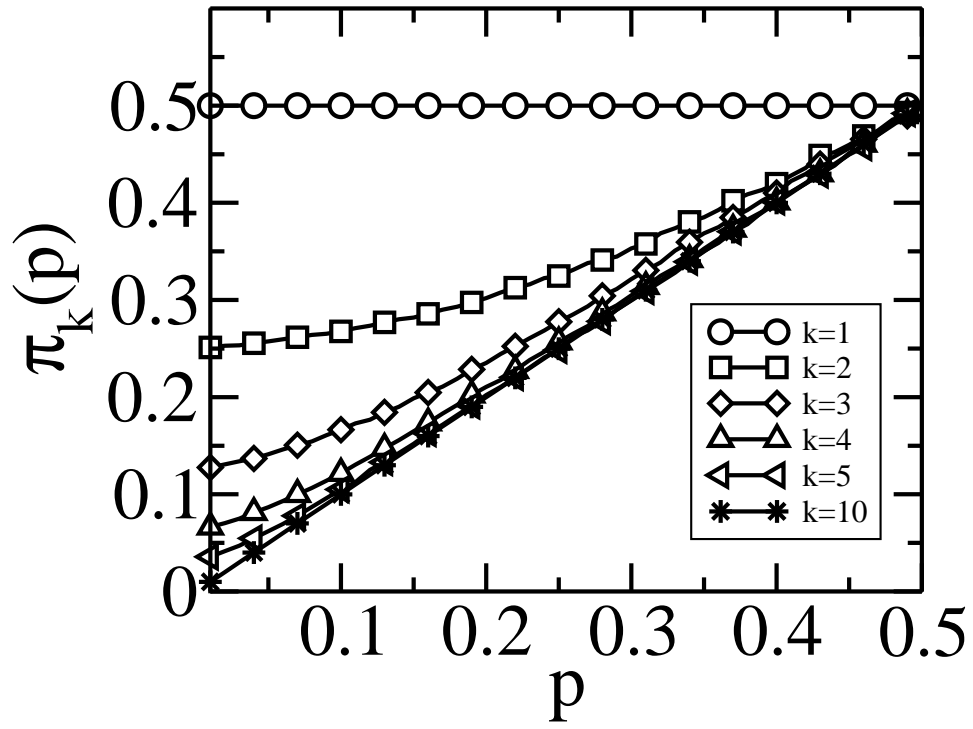


Figure 7:

	RF	CF	NCF	SNCF
E1	1.9	1.8	1.8	1.7
E2	1.6	1.6	1.6	1.5
E2*	1.7	1.6	1.7	1.6
Yeast	4.8	4.2	4.1	3.4

Table 1:






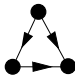

							
	(a)	(b)	(c)	(d)	(e)	(f)	(g)
Yeast (%)	35	31	20	4.8	4.0	3.5	0.2
E1 (%)	41 ± 2	28 ± 3	23 ± 1	1.8 ± 0.8	2.5 ± 1.1	2.5 ± 0.5	0.1 ± 0.1
E2 (%)	37 ± 2	30 ± 3	25 ± 2	1.4 ± 0.6	1.7 ± 0.7	3.1 ± 0.5	0.04 ± 0.07

Table 2: